

COMPARABLE PERFORMANCE EVALUATION OF HC AND HFC REFRIGERANTS IN AN OPTIMIZED SYSTEM

PIOTR A. DOMANSKI^(a), DAVID YASHAR^(b)

National Institute of Standards and Technology

100 Bureau Drive, Stop 8631

Gaithersburg, MD 20899-8631, USA

^(a)piotr.domanski@nist.gov, ^(b)david.yashar@nist.gov

ABSTRACT

This paper presents an analytical evaluation of isobutane (R600a), propane (R290), R134a, R22, R410A, and R32 in a vapor compression system used for comfort cooling applications. The evaluation method was based on a system simulation model that was complimented with an evolutionary computation module for the optimization of refrigerant circuitries in the evaporator and condenser. The evaluation showed the coefficient of performance (COP) for the studied refrigerants to be within 13 %, with R32 and R290 having the highest system COPs. This evaluation produced a vastly different ranking of the compared fluids than that obtained from a theoretical cycle analysis based on thermodynamic properties alone. In the system simulations, the high pressure refrigerants overcame the thermodynamic disadvantage associated with their low critical temperature and had higher COPs than the low-pressure R134a and R600a, which were ranked the highest by the thermodynamic cycle analysis. The presented results include entropy generation information for complete systems and individual system components.

1. INTRODUCTION

Increased concerns about climate change prompted numerous studies comparing the performance of hydrofluorocarbon (HFC), hydrocarbon (HC), carbon dioxide and other natural refrigerants in various applications. In some cases, the results from different studies are conflicting. This problem is not new. Inconsistent results can be found in the literature from the previous decade when HFCs were compared to chlorine-containing refrigerants.

A number of methodologies can be used for evaluating competing refrigerants. A first-order comparison can be obtained through theoretical analysis based on thermodynamic properties alone, e.g., using the CYCLE_D program (Domanski et al., 2003). While this type of evaluation may include effects such as refrigerant pressure drops in heat exchangers, evaporator superheat, condenser subcooling, or even the temperature difference between fluids exchanging heat, they do not involve transport properties, and this is their major shortcoming. More involved analytical methods include both thermodynamic and transport properties, and may be implemented through simulation models of various complexities.

When comparing different refrigerants through a laboratory experiment, it is important to assure that all system components are optimized for each individual refrigerant (or to take corrective measures) because the refrigerant's performance in a system is strongly affected by hardware design. Certainly, so called drop-in tests, where different refrigerants are tested in the same unmodified system, do not yield suitable information for comparing the potentials of different refrigerants since different refrigerants provide different cooling capacities and require different saturation temperatures in the heat exchangers. Also, results from tests in a so called breadboard

apparatus equipped with a variable-speed compressor can provide biased results. Although, modulation of the compressor speed allows adjustment of the system capacity for each refrigerant to the same value, the unchanged designs of evaporator, condenser, and connection tubing will affect fair performance comparison.

A fair comparison of the performance merits of different refrigerants for a given application requires systems in which all components are optimized for the given refrigerant. Selecting a suitable expansion device presents no difficulty, while some care is needed to specify appropriate connection tubes. A more challenging task is to provide heat exchangers and compressors that are optimized individually for each refrigerant. In particular, providing optimized compressors may prove to be the most difficult task because the compressors should be sized properly to assure equal cooling capacity for each system.

A study on the performance of propane (R-290), R-404A and R-410A combined computer simulations and laboratory measurements (Hwang et al., 2004). The authors optimized condenser circuitries for each refrigerant using computer simulations. In the final analysis they modified their laboratory measurements by using the same compressor isentropic efficiency for all three refrigerants. The researchers used the same evaporator with the assumption that it is the least sensitive component of a system used in the medium temperature refrigeration application they studied.

The goal of this analytical study is to evaluate the relative performance of R600a (isobutane), R290, R134a, R22, R410A, and R32 in a comfort cooling application with the emphasis on optimization of the heat exchanger circuitries. This study follows the studies of optimized finned-tube evaporators (Domanski et al., 2005) and condensers (Domanski and Yashar, 2005).

2. STUDIED REFRIGERANTS

Table 1 presents the refrigerants used in this study. They represent a wide range of thermophysical properties that affect heat exchanger and system performance. Differences in thermodynamic properties of the studied refrigerants can be visually recognized on a temperature-entropy diagram, as shown in Figure 1 with the entropy scale normalized for qualitative comparison. The shown two-phase domes are significantly different, which is chiefly due to different critical temperatures and molar specific heats.

Regarding evaporator and condenser performance, the critical temperature influences refrigerant pressure, vapor density, and the change of saturation temperature with respect to pressure drop, which are important parameters for heat exchanger design. Among transport properties, liquid thermal conductivity and liquid viscosity are the most important. Figure 2 presents these properties for the studied refrigerants relative to the corresponding properties of R22.

Table 1. Refrigerant Information⁽¹⁾

Refrigerant	Saturated Vapor Pressure ⁽²⁾ (kPa)	Molar Mass (g mol ⁻¹)	Molar Vapor Specific Heat ^(2,3) (J mol ⁻¹ K ⁻¹)	Safety Designation ⁽⁴⁾	GWP ⁽⁵⁾ (100 years horizon) ⁽⁶⁾
R600a	199.5	58.122	97.79	A3	20
R134a	374.6	102.03	94.93	A1	1320
R290	584.4	44.096	81.88	A3	20
R22	621.5	86.468	66.63	A1	1780
R410A	995.0	72.585	87.27	A1/A1	2000
R32	1011.5	52.024	69.16	A2	543

⁽¹⁾ All fluid properties based REFPROP (Lemmon et al., 2002); ⁽²⁾ correspond to 7.0 °C dew-point temperature;

⁽³⁾ at constant pressure; ⁽⁴⁾ (ASHRAE, 2001); ⁽⁵⁾ Global Warming Potential; ⁽⁶⁾ (Calm and Hourahan, 2001; IPCC, 2001)

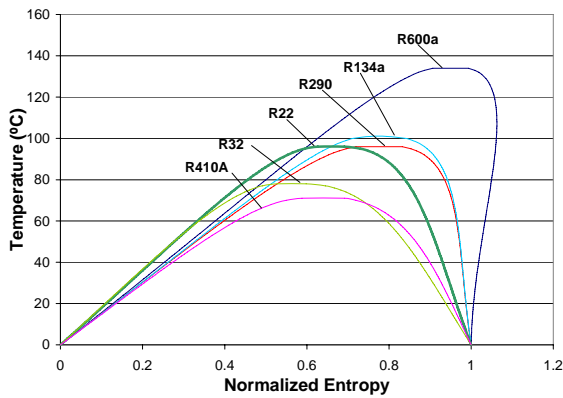


Figure 1. Temperature - Entropy diagram for studied refrigerants (Entropy is normalized to the width of the two-phase dome.)

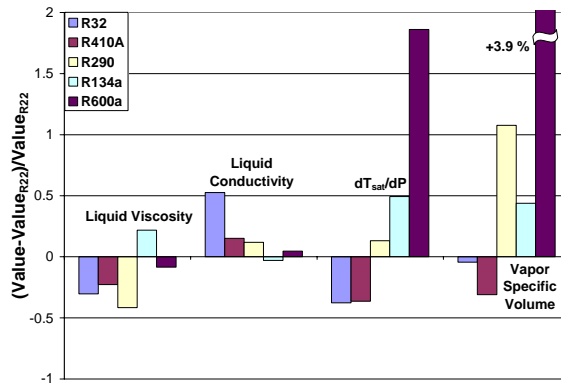


Figure 2. Thermophysical properties of selected refrigerants relative to R22 properties at 7 °C

3. SELECTED SYSTEMS

We elected to use an R22 system as a basis for comparison in this study. The first task was to set up the constraints for the reference R22 system and select its components. We assumed that at the 35 °C rating condition our reference R22 system will operate at the evaporator exit saturation temperature of 7.0 °C and the condenser inlet saturation temperature of 45.0 °C. We also assumed that the evaporator exit superheat and condenser exit subcooling will be 5 °C. The system did not include the connecting tubes to eliminate the influence of their sizing on the system performance.

We used the above refrigerant state constraints to specify R22 system components: evaporator, condenser, and compressor. For the R22 evaporator, as well as for the other refrigerants, we selected the 3-depth row coils studied and optimized by Domanski et al. (2004). Table 2 presents the design information for the evaporators, and Figure 3 shows the three types of optimized circuitry architectures; 1.5-circuit for R32, R410A, R290, R22; 3-circuit for R134a; and 4-circuit for R600a.

The refrigerant circuitries were optimized using an evolutionary module ISHED (Intelligent

System for Heat Exchanger Designs, Domanski et al., 2004a). ISHED consists of a heat exchanger simulator (evaporator or condenser simulation model), which provides capacities of heat exchangers with different circuitry architectures, and a set of modules which participate in the preparation of the new architectures. ISHED uses the conventional evolutionary approach in that it operates on one generation (population) of circuitry architectures at a time. Each member of the population is evaluated by the heat exchanger simulator, which provides the heat exchangers' capacity as a single numerical fitness value. The designs and their fitness values are returned to ISHED's Control Module as an input for deriving

Table 2. Evaporator design information

Items	Unit	Value
Number of depth rows		3
Number of tubes per row		12
Tube length	mm	500
Tube pitch	mm	25.4
Tube depth row pitch	mm	22.2
Tube inside diameter	mm	9.2
Tube outside diameter	mm	10.0
Fin thickness	mm	0.2
Fin pitch	mm	2
Tube inner surface		smooth
Fin geometry		louver
Tube material		copper
Fin material		aluminum
Face air velocity (uniform)	m s ⁻¹	3.0

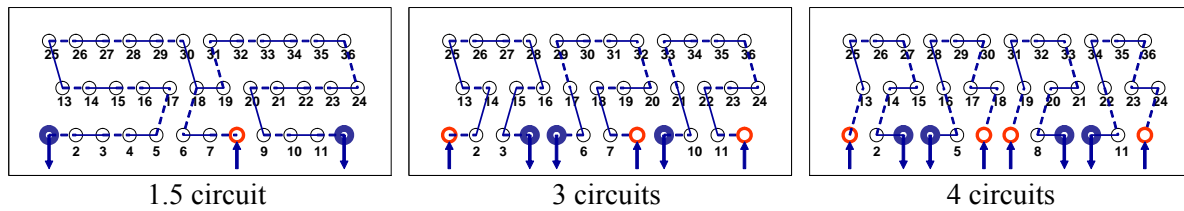


Figure 3. ISHED optimized evaporator circuitry designs; 1.5 circuit for R32, R410A, R22, and R290, 3 circuits for R134a, and 4 circuits for R600a. Air flows vertically from the bottom to the top. (Domanski et al. 2004)

the next generation of circuitry designs. Typically, several thousand refrigerant circuitries are evaluated during a single optimization run. The application of ISHED to optimizing finned-tube evaporators and condenser for uniform and non-uniform air velocity profiles is presented in Domanski et al. 2004 and Domanski and Yashar (2005), respectively.

We selected the reference R22 condenser during optimization runs using 45 °C condenser inlet saturation temperature and 5 °C subcooling. Table 3 presents the condenser specifications. All parameters listed in the table were pre-specified except the tube length. During optimization runs, the circuitry of an R22 condenser with the approximate tube length was optimized using ISHED. Then the optimized architecture was simulated with the refrigerant mass flow rate fixed to that found in the corresponding evaporator study. Condenser tube length (and therefore the air volumetric flow rate) was adjusted until the target 5 °C subcooling resulted at the condenser exit.

Once the size of the R22 condenser was determined, we carried out circuitry optimization simulations for other refrigerants using ISHED. The refrigerant inlet state to the condenser was defined by the 45 °C saturation temperature, and the compression process isentropic efficiency of 0.70 that originated at the evaporator exit saturation temperature of 7.0 °C with 5.0 °C superheat. This approach of determining the refrigerant inlet state to the condenser was used previously (Casson et. al., 2002). Table 4 shows condenser inlet pressure, temperature, and superheat for the six refrigerants.

Table 3. Condenser Design Information

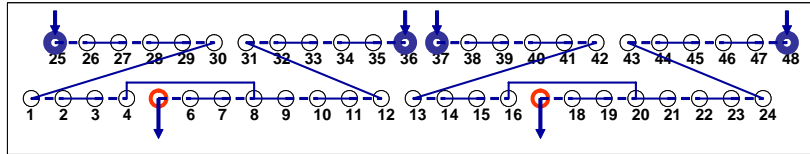
Number of depth rows	Unit	2
Number of tubes per row		24
Tube length	mm	1728
Tube inside diameter	mm	7.7
Tube pitch	mm	25.4
Tube depth row pitch	mm	22.2
Tube outside diameter	mm	8.3
Fin thickness	mm	0.2
Fin pitch	mm	2.0
Tube inner surface		smooth
Fin geometry		lanced
Tube material		copper
Fin material		aluminum
Face air velocity (uniform)	m s ⁻¹	1.0

Table 4. Condenser Inlet Refrigerant State

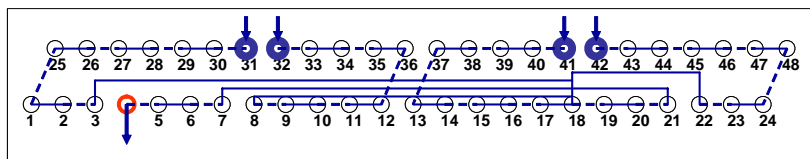
Refrigerant	Pressure (kPa)	Superheat (°C)	Temperature (°C)
R600a	604.2	9.8	54.8
R134a	1159.9	17.9	62.9
R290	1534.4	17.01	62.1
R22	1729.2	33.8	78.8
R410A	2726.2	30.23	75.2
R32	2794.8	47.2	92.2

ISHED returned two different designs for the six refrigerants studied. Figure 4 shows two optimized condenser circuitries from ISHED and one well performing manually generated design (with four circuits merging into one outlet) that is outside the domain of possible designs for ISHED at this time. Figure 5 shows the capacities of these three condensers with each

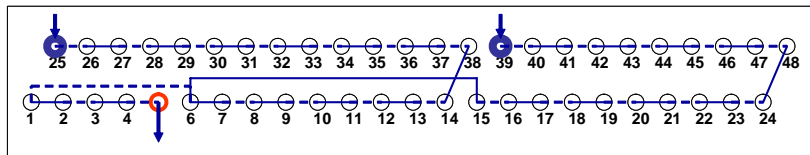
refrigerant at the design conditions. During the optimization runs ISHED employed EVAP-COND's evaporator and condenser simulation modules (NIST, 2006). The following refrigerant-side correlations were used: the Thome correlation for flow boiling heat transfer (Thome, 2004), the Hajal/Thome/Cavallini correlation for condensation heat transfer (Hajal et al., 2003), and the Müller-Steinhagen/Heck correlation for two-phase pressure drop (Müller-Steinhagen and Heck, 1986). Thermophysical properties of refrigerants were calculated using REFPROP's routines (Lemmon et al., 2002).



Design A: ISHED generated condenser design used for R600a



Design B: Manually generated condenser design used for R134a, R290, R22, and R410A



Design C: ISHED generated condenser design used for R32

Figure 4. Condenser circuitry designs. Air flows vertically from the bottom to the top.

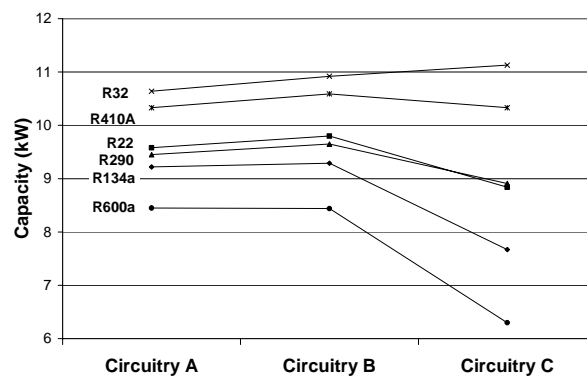


Figure 5. Capacities of condensers with different refrigerant circuitries

4. SYSTEM SIMULATIONS AND RESULTS

We performed simulations using a system simulation model ACSIM, which is comprised of EVAP-COND heat exchanger models and a compressor simulation module based on compressor maps (ARI, 2004). We used performance maps of a commercially available R22 compressor as the reference performance characteristics for the compressors for all six fluids. We implemented two options to the compressor simulation module:

- A correction parameter for modifying the predicted refrigerant mass flow rate, input by the program user. Its use is equivalent to adjusting compressor volumetric capacity.
- Use of the R22 compressor performance maps for other refrigerants. Under this option, the compressor module calculated the refrigerant volumetric flow rate and isentropic efficiency for the R22 compressor based on the saturation temperatures at compressor suction and discharge. Then compressor power and refrigerant mass flow rate were calculated using thermodynamic properties of the studied refrigerant.

We performed simulations at outdoor air operating conditions of 35.0 °C dry bulb temperature with 50 % relative humidity and 101.325 kPa pressure. The indoor air condition was 26.7 °C dry-bulb temperature with 50 % relative humidity and 101.325 kPa pressure.

Simulations started with the reference R22 system. We set the compressor mass flow adjusting parameter to obtain the evaporator exit saturation temperature of 7.0 °C. This simulation run provided the nominal reference capacity for all refrigerants at the 35 °C operating condition. For the subsequent simulations with other refrigerants, we set the compressor mass flow rate adjusting parameter to obtain the R22 reference capacity. Depending on the refrigerant, this resulted in an increased evaporator saturation temperature and decreased condenser saturation temperature, or vice versa. An increased or decreased temperature lift changed the compressor isentropic efficiency for a given case as compared to that obtained by the R22 system.

In addition to the air-conditioning system simulations using ACSIM, we used CYCLE_D (Domanski et al., 2004) to carry out theoretical thermodynamic cycle simulations. For each refrigerant we used the R22 system saturation temperatures in the evaporator and condenser, 5.0 °C evaporator superheat, 5.0 °C condenser subcooling, and a compressor isentropic efficiency of 0.70. Figure 6 and Table 5 present results of the cycle and system simulations. For the theoretical simulations, as expected, the relative COPs of refrigerants are in descending order of their critical temperatures. For system simulations with optimized heat exchangers, the high pressure refrigerants overcame the theoretical disadvantage and provided the highest operating efficiency. The low pressure refrigerants, R600a and R134a, had a somewhat lower sensible heat ratio than the remaining refrigerants, i.e., they had a higher latent capacity. The compressor isentropic efficiency varied by less than 1 % due to temperature lift.

Figure 7 provides complementary entropy generation information for the studied refrigerants. The expansion device and compressor were adiabatic components in this study. The air was

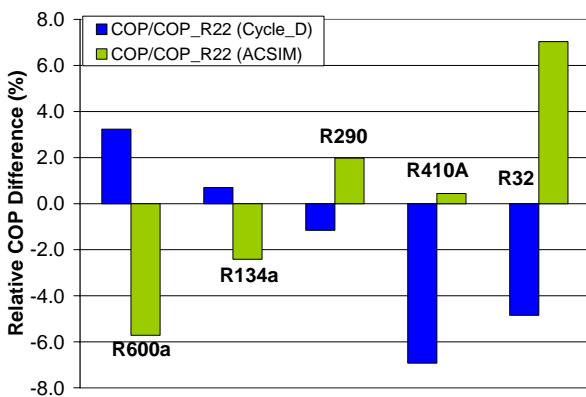


Figure 6. COP differences referenced to COP for R22 from theoretical cycle simulations and system simulations

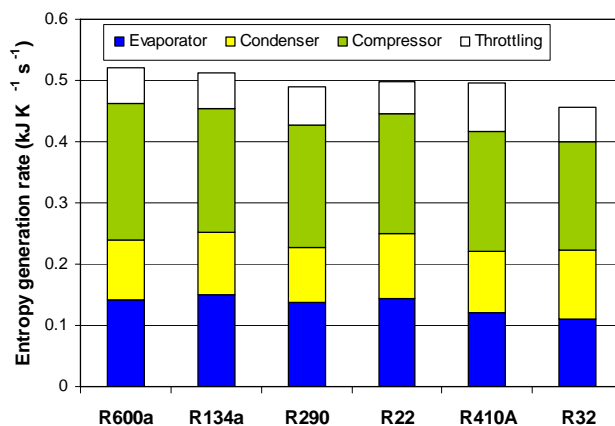


Figure 7. Entropy generation rate per 1 kW of cooling capacity

Table 5. Selected results from air conditioner simulation

Refrigerant	Sensible heat ratio ^(a)	Evaporator		Condenser		Compressor isentropic efficiency
		$T_{\text{sat, out}}$ (°C)	$T_{\text{sat, drop}}$ (°C)	$T_{\text{sat, in}}$ (°C)	$T_{\text{sat, drop}}$ (°C)	
R600a	0.78	6.0	2.5	46.6	2.2	0.698
R134a	0.78	6.5	2.6	45.6	2.2	0.701
R290	0.80	8.1	2.1	45.3	1.2	0.705
R22	0.80	7.0	3.8	45.1	1.4	0.702
R410A	0.80	8.5	1.7	44.6	0.8	0.706
R32	0.80	9.1	1.0	44.1	1.1	0.707

^(a)The ratio of sensitive capacity and total capacity

considered as a two component mixture to account for the entropy change during the dehumidification process.

The presented results are applicable to the system using heat exchangers where the refrigerant-side heat transfer mechanism is based on forced convection evaporation and condensation, and are not applicable to systems with shell-and-tube type heat exchanger where pool boiling and space condensation take place. The results will vary with the variations of the relative resistances of the refrigerant and air sides.

5. CONCLUDING REMARKS

The heat exchanger optimization results with the ISHED package show that the optimization process of finned-tube heat exchangers has a set of rather discreet solution options. In our case, R290, R22, R410A and R32 used the same optimized evaporator, while R22, R290, R134a, R410A used the same condenser.

The evaluation of performance of R600a, R290, R134a, R22, R410A, and R32 in systems with optimized heat exchangers showed the COP for the studied refrigerant to be within 13 %, with R32 and R290 having the highest COP. This evaluation produced a vastly different ranking of the compared fluids than that obtained from a theoretical cycle analysis based on thermodynamic properties alone. In the system simulations, the high pressure refrigerants overcame the thermodynamic disadvantage associated with their low critical temperature and had higher COPs than the low pressure R134a and R600a. Although the presented evaluation methodology is based on simulations alone, we expect it to provide a fair indication of performance of different fluids on a relative basis. This approach may be followed with experimental effort if stronger credentials are desired. Still, such a COP ranking is only a preliminary step in a refrigerant selection process that should include the life cycle climate performance for a given cost required to put air-conditioning equipment on the market.

NOMENCLATURE

COP – coefficient of performance

P – pressure, kPa

T_{sat} – dew-point temperature, °C (Fig. 2)

$T_{\text{sat, drop}}$ – change in refrigerant saturation temperature, °C

$T_{\text{sat, in}}$ – refrigerant saturation temperature at evaporator inlet, °C

$T_{\text{sat, out}}$ – refrigerant saturation temperature at evaporator inlet, °C

REFERENCES

- ARI. 2004, Performance Rating of Positive Displacement Refrigerant Compressors and Compressor Units, Std. 540-2004, Air-Conditioning and Refrigeration Institute, Arlington, VA, USA.
- ASHRAE, 2001, *ANSI/ASHRAE Standard 34-2001; Designation and safety classification of refrigerants*. American Society of Heating, Refrigerating, and Air-conditioning Engineers, Atlanta, GA, USA.
- Calm, J.M. and Hourahan, G.C. 2001, Refrigerant data summary. *Engineered Systems*, 18(11): 74-88.
- Casson V, Cavallini A, Cecchinato L, Del Col D, Doretti L, Fornasieri E, Rossetto L, Zilio C. 2002, Performance of finned coil condensers optimized for new HFC refrigerants. *ASHRAE Transactions* 2002;108(2): pp.517-527.
- Domanski PA, Didion DA, Chi J. 2003, NIST Vapor Compression Cycle Design Program – CYCLE_D 3.0. Standard Reference Database 49, National Institute of Standards and Technology, Gaithersburg, MD.
- Domanski, P.A., Yashar, D. 2005, Optimization of Finned-Tube Condensers Using an Intelligent System, IIR Commission B1/B2 Conference, Thermophysical Properties and Transfer Processes of Refrigerants, Vicenza, Italy, Aug 31 – Sept. 2.
- Domanski, P.A., Yashar, D., Kaufman, KA., Michalski R.S. 2004, Optimized design of finned-tube evaporators using learnable evolution methods. *Int. J. HVAC&R Research*, 10(2): 201-212.
- Domanski, P.A., Yashar, D., Kim, M. 2005, Performance of a finned-tube evaporator optimized for different refrigerants and its effect on system efficiency, *Int. J. Refrig.*, 28 (6): 820-827.
- Hajal, J.E., Thome JR, Cavallini A. 2003, Condensation in horizontal tubes, part II: new heat transfer model based on flow regime, *International Journal of Heat Mass Transfer*; 46(18): 3365-3387.
- Hwang, Y., Jin, D-H, Radermacher, R. 2004, Comparison of Hydrocarbon R-290 and two HFC Blends R410A and R404A for Medium Temperature Refrigeration Applications, Global Refrigerant Environmental Evaluation Network (GREEN) Program, Air-Conditioning and Refrigeration Institute, Arlington VA, USA
- IPCC. 2001, *Climate change 2001: The scientific basis – Contribution of working group I to the IPCC third assessment report*. Intergovernmental Panel on Climate Change of the World Meteorological Organization and the United Nations Environment Programme (UNEP); Cambridge, UK. Cambridge University Press.
- Lemmon, E.W., McLinden, M.O., Huber, M.L. 2002, NIST Reference Fluids Thermo-dynamic and Transport Properties – REFPROP 7.0. Standard Reference Database 23, National Institute of Standards and Technology, Gaithersburg, MD, USA.
- Müller-Steinhagen H, Heck K. 1986, A simple friction pressure drop correlation for two-phase flow in pipes, *Chem Eng Process* 1986;20(6): 297-308.
- NIST. 2006, EVAP-COND - Simulation models for finned-tube heat exchangers, Version 2. National Institute of Standards and Technology, Gaithersburg, MD, USA.
<http://www2.bfrl.nist.gov/software/evap-cond/>
- Thome, J. R. 2005, Update on advances in flow pattern based two-phase heat transfer models, *Experimental Thermal and Fluid Science*, v 29, n 3: 341-349.